Analytical Modeling of the Base Dark Saturation Current of Drift-Field Solar Cells Considering Auger Recombination

Md. Rashedul Huqe*‡, Sahajadee Islam Reba**, Md. Shihab Uddin**, Md. Iqbal Bahar Chowdhury**

*United International University, Centre for Energy Research, Dhaka, Bangladesh.

**United International University, Department of Electrical and Electronic Engineering, Dhaka, Bangladesh.

rashedul_uiu@yahoo.com, rebaa.islam@gmail.com, msu.uiu.eee@gmail.com, ibchy@eee.uiu.ac.bd

‡Corresponding Author: United International University, House# 80, Road#8/A, Shatmasjid Road, Dhaka-1209, Bangladesh.

+8801914456709, E-mail: rashedul_uiu@yahoo.com

Received: 15.04.2013 Accepted: 28.05.2013

Abstract-In this work, an analytical model has been developed for the dark saturation current in the heavily-doped base region of a drift-field Si-solar cell. Unlike the conventional models available in the literature, this model incorporates both the SRH (Shockley-Read-Hall) and the Auger recombination mechanisms in the base. The mathematical intractability due to this consideration has been resolved by using an elegant exponential approximation technique. The simulations carried out by the developed model shows that the Auger recombination becomes significant even for a 1 μm wide base when surface recombination velocity is lowered to the order of 10^4 *cm/s* and/or when the doping level is of the order of 10^{19} cm^{-3}.

Keywords-Drift-Field Solar Cell, Dark Saturation Current, SRH Recombination, Auger Recombination, Non-uniformly Doped Base.

1. Introduction

The concept of a drift-field (DF) solar cell [1] is to introduce electric fields in the bulk emitter and base regions in the same direction as that developed in the depletion region. These fields decrease the retarding current due to forward-biased diode action. As a result, the DF solar cells have higher conversion efficiency than that of the conventional solar cells. The conversion efficiency of the DF solar cells can be made even higher by increasing the strength of these developed fields i.e. by increasing the doping level so that the logarithmic slope of the doping profile can be made higher. However, use of increasingly heavy doping levels not only results in the dominance of the Auger recombination but also invokes several non-ideal effects which include the band-gap narrowing effect and the position dependency of the carrier transport parameters (i.e. mobility and lifetime). Till to date, a number of research works [2-7] have been carried out to incorporate these effects in the modeling of dark saturation current. The model of Bullis [2] assumed uniform mobility; Kaye *et al.* [3] and Overstraeten *et al.* [4] considered linear position dependency of carrier mobility; Lindholm & Chen's [5] model incorporates the doping dependent carrier lifetime only. Verhoff and Sinke [6] considered the doping dependence of both carrier mobility and lifetime. But, for lifetime, they considered the SRH and Auger recombination separately, not simultaneously; they considered Auger recombination for doping level $\geq 5\times10^{18}$ cm^{-3} and SRH recombination for lower doping levels. Therefore, their model suffers from accuracy problem.

In this work, both the SRH and the Auger recombination as well as all the non-ideal effects mentioned earlier in this section are incorporated in the model derivation. The resulting mathematical intractability due to simultaneous consideration of SRH and Auger recombination has been resolved by applying an elegant exponential approximation technique. Simulations are carried out using the developed model to investigate the effects of simultaneous consideration of both SRH and Auger recombination.

2. Analysis

The basic equations required for the p-type base region of a drift solar cell are

$$J_n = qn(x)\mu_n(x)E(x) + qD_n(x)\frac{dn(x)}{dx} \quad (1)$$

$$\frac{dJ_n}{dx} = q(R-G) \quad (2)$$

where μ_n and D_n are the mobility and the diffusivity of electrons, $R_n - G_n$ is the net recombination rate and $E(x)$ is the electric field acting on the electron caused by the non uniform doping profile. Considering the band gap narrowing (BGN) effects due to heavy doping level, the electric field $E(x)$ can be expressed as [8]

$$\frac{E}{V_T} = \frac{d}{dx} ln\, N_a(x) - \frac{d}{dx} ln\, n_{ie}^2(x) \quad (3)$$

where $V_T = \frac{KT}{q}$ is the thermal voltage and n_{ie} is the effective intrinsic carrier concentration due to BGN effects given by [9]

$$n_{ie}^2(x) = n_{i0}^2\left[\frac{N_a(x)}{N_{0,ref}}\right]^{\gamma_2} \quad (4)$$

where $n_{i0} = 1.194 \times 10^{10} cm^{-3}$, $N_{0,ref} = 1.3\times10^{17}\, cm^{-3}$ and $\gamma_2 = 0.5355$. For practical doping density ranges, electron mobility μ_n becomes doping dependent. This doping dependency can be approximated as [6]

$$\mu_n = \frac{qD_n(0)}{kT}\left[\frac{N_a(x)}{N_{m,ref}}\right]^{-\gamma_1} \quad (5)$$

With $D_n(0)$ = 20.72 cm^2 (V-s)$^{-1}$, $N_{m,ref} = 1\times10^{17} cm^{-3}$ and $\gamma_1 = 0.42$. For heavily doped silicon, the band-to-band Auger recombination involving direct transitions and SRH recombination through traps are significant. Under steady-state condition, these recombination rates are given by

$$R_{SRH} = \frac{n}{\tau_{ns}} \quad (6)$$

$$R_{Auger} = \frac{n}{\tau_{na}} \quad (7)$$

where τ_{ns}, τ_{na} are the doping-dependent electron lifetime for SRH recombination [10, 11] and Auger recombination [12], respectively and can be expressed as

$$\tau_{ns} = \frac{\tau_{n0}}{1+\frac{N_a}{N_{0,ref}}} \quad (8)$$

$$\tau_{na} = \frac{1}{C_{Ap}N_a^2} \quad (9)$$

Where $N_{0,ref}$ = 7.1 × 10^{15} cm^{-3} and $\tau_{n0} = 3.95\times10^{-4}\, sec$ [11] and C_{Ap} is the Auger coefficient for electrons given by [12]

$$C_{Ap} = 0.72\times10^{-31} - 0.15\times10^{-34}T + 2.92\times10^{-37}T^2$$

The total recombination rate R_n in the base region can be expressed as

$$R_n = \frac{n}{\tau_{n,eff}} \quad (10)$$

where $\tau_{n,eff}$ is the effective electron life time given by

$$\frac{1}{\tau_{n,eff}} = \frac{\tau_{n0}}{1+\frac{N_a}{N_{0,ref}}} + C_{Ap}N_a^2 \quad (11)$$

Under the dark condition, the generation rate G_n is zero. Therefore, the electron current continuity equation given by Eqn. (2) can be rearranged as

$$\frac{dJ_n}{dx} = \frac{qn}{\tau_{n,eff}} \quad (12)$$

3. Model Derivation

Differentiating Eqn. (1) with respect to x, combining with Eqn. (12) and then rearranging, results in a second order differential equation (DE) of n(x) as

$$\frac{d^2n}{dx^2} + \left[\frac{E}{V_T} - \frac{d}{dx}ln\left(\frac{1}{qD_n}\right)\right]\frac{dn}{dx} + \left[\frac{d}{dx}\left(\frac{E}{V_T}\right) - \frac{E}{V_T}\frac{d}{dx}ln\left(\frac{1}{qD_n}\right) - \frac{1}{\tau_{n,eff}D_n}\right]n = 0 \quad (13)$$

Since the electric field, the mobility and the lifetime- all depend on the type of the doping profile, the solution of the above-mentioned DE can be obtained, provided that the doping profile in the base region is specified. In this work, the base doping profile is considered as exponential which can be expressed as

$$N_a(x) = N_a(0)u(x) = N_a(0)e^{\frac{\eta x}{W_b}} \quad (14)$$

where u is a convenient variable, W_b is the base width, $\eta = log\left[\frac{N_a(0)}{N_a(W_b)}\right]$ is the logarithmic slope of the doping profile and $N_a(0)$ and $N_a(W_b)$ are the doping densities at the edge of the junction i.e. at $x = 0$ and at the surface side of the base i.e. at $x = W_b$

For the exponential profile, the electric field, the carrier mobility and the lifetimes for SRH and Auger recombination can be arranged as

$$\frac{E}{V_T} = \frac{\eta}{W_b}(1-\gamma_2) \tag{15}$$

$$\frac{1}{qD_n} = \frac{1}{qD_n(0)}\left[\frac{N_a(0)}{N_{0ref}}\right]^{\gamma_1} u^{\gamma_1} = F_e u^{\gamma_1} \tag{16}$$

$$\frac{1}{\tau_{ns}} \approx \frac{1}{\tau_{n0}}\frac{N_a(0)}{N_{0ref}} u = R_{ns} u \tag{17}$$

$$\frac{1}{\tau_{na}} = C_{Ap}[N_a(0)]^2 u^2 = R_{na} u^2 \tag{18}$$

Therefore, for the exponential doping profile,' the DE [Eqn. 13] can be organized as

$$\frac{d^2 n}{dx^2} + G_1 \frac{dn}{dx} + G_2 n = 0 \tag{19}$$

where

$$G_1 = -\frac{\eta}{W_b}(1-\gamma_2-\gamma_1)$$

$$G_2 = -\left[\left(\frac{\eta}{W_b}\right)^2 \gamma_1(1-\gamma_2) + F_e(R_{ns}u + R_{na}u^2)u^{\gamma_1}\right]$$

The analytical intractability of this DE is due to the second term of G_2. Verhoff and Sinke [6] solved this DE by separately considering the SRH and Auger recombination i.e. they used either $R_{ps}u$ or $R_{pa}u^2$. In this work, using the exponential approximation technique [described in Appendix A], the term $\frac{1}{\tau_{n,eff} D_n}$ can be approximated as a simple exponential given by

$$\frac{1}{\tau_{n,eff} D_n} \equiv R_0 u^{k_n} \tag{20}$$

where R_0 and k_n can be obtained using the relations given in Appendix A. The solution of (Eqn. 19) i.e. minority electron concentration, n(x) can be expressed as a combination of modified Bessel functions of first and second kind [I_β and K_β] of order β as [Appendix B]

$$n(x) = w(x)[C_1 y_1(x) + C_2 y_2(x)] \tag{21}$$

where all the variables and constants are defined in the Appendix B. The electron current density $J_n(x)$ in the base region can be obtained from the electron current equation [Eqn. (1)] and taking the value of J_n at $x = 0$ gives

$$J_n(0) = J_0 e^{\frac{qV_L}{KT}} \tag{22}$$

where J_0 is the base dark saturation current given by

$$J_0 = \frac{qD_{n0}n(0)}{\alpha_0}[\beta + X_0 r_0] \tag{23}$$

where $r(x) = \frac{d}{dx}\ln[y_1(x) - \beta_s y_2(x)]$, $\beta = \frac{1-\gamma_2+\gamma_1}{k_n}$, $\alpha_0 = \frac{2W_b}{\eta k_n}$, and subscript '0' denotes the value at $x = 0$.

4. Results and Discussion

This section presents the simulation results obtained from the model developed in this work and also, gives a physics-based analysis on these results.

Volume recombination in the Si-base region includes both SRH and Auger recombination mechanisms. Since, at present, heavy doping levels ($>10^{18}\ cm^{-3}$) are commonly used in the base region, Auger recombination should be more probable than the SRH recombination. Moreover, since the dark saturation current J_0 needs to make up the carrier loss caused by the volume recombination in the base region, J_0 has to be higher when considering both SRH and Auger recombination than that considering only the SRH or the Auger recombination and also, J_0 considering only the Auger recombination should be higher than that considering only the SRH recombination, provided that the base doping level is excessive. It is evident that Figs. (1), (2) and (3) are in accordance with the above-mentioned statements.

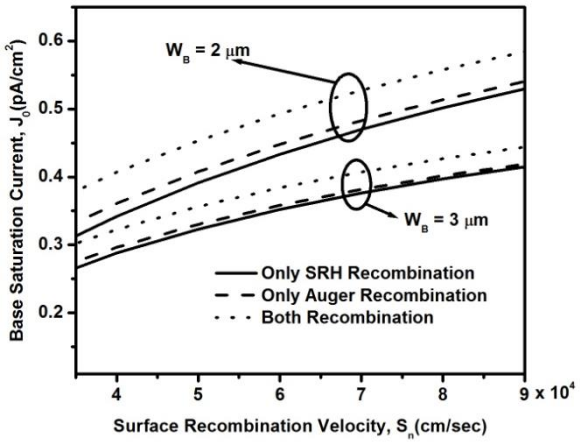

Figure 1: Effect of the variation of surface recombination velocity on the base saturation current density J_0 for two values of base width (W_B = 2 μm and 3 μm). Here, $N_a(W_B) = 4 \times 10^{19}$ cm^{-3}.

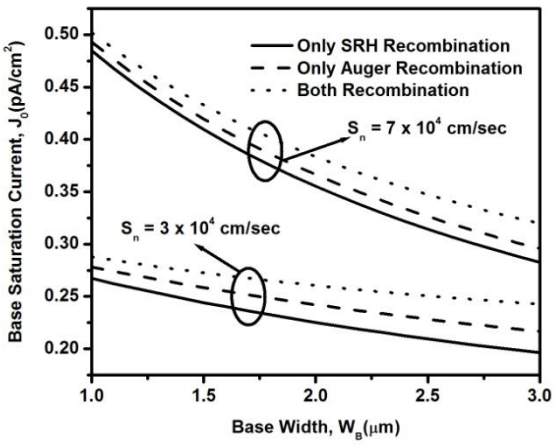

Figure 2: Effect of the variation of base width on the base Saturation current density J_0 for two values of surface recombination velocity ($S_n = 3\times10^4$ cm/secand 7×10^4 cm/sec). Here, $N_a(W_B) = 5\times10^{19}\ cm^{-3}$.

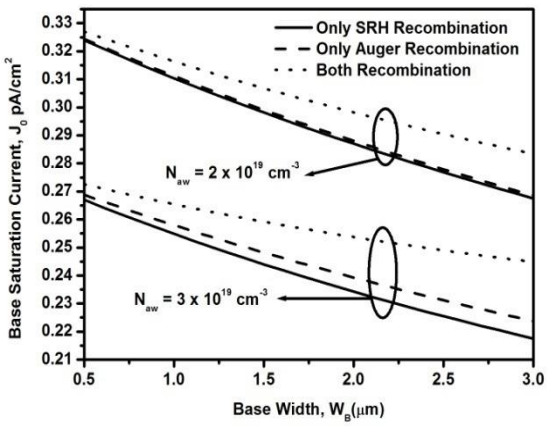

Figure 3: Effect of the variation of base width on the base Saturation current density J_0 for two values of peak doping concentration [$N_a(W_B) = 2\times10^{19}$ cm^{-3} and 3×10^{19} cm^{-3}]. Here, $S_n = 2\times10^4\ cm/sec$

Since the surface recombination velocity S_n represents the amount of surface defects at the edge of the base side of the solar cells, increase in S_n means increase in the defects and hence, increased carrier losses at the base surface. In order to make up this carrier lose at the surface, the dark saturation current J_0 has to increase. This fact is evidenced from the Figs. (1) and (2).

The dark saturation current in the base region flows from its junction side to the surface side. Due to the volume recombination in the base region, the current at the junction side is decreased from the surface side. Increase in base width (W_B), therefore, results in more lowering of the current at the junction side. Since J_0 is conventionally calculated at the junction side, the increase of the base width causes J_0 to decrease. From Figs. (1), (2) and (3), this trend of J_0 against W_B is reflected.

When peak base doping level $N_a(W_B)$ is increased keeping $N_a(0)$ constant, the electric field in the base region is increased due to the increase in the logarithmic gradient of the doping profile. On the other hand, this increase in $N_a(W_B)$ results in the increase of carrier population throughout the base region which, in turn, decreases the carrier mobility according to a power law [Eqn. (5)]. Therefore, the decrease in the carrier mobility dominates over the increase in the electric field when $N_a(W_B)$ is increased keeping $N_a(0)$ constant and hence, under such condition, J_0 gets decreasing. Figure (3) also supports this fact.

A close observation of the Figs. (1), (2) and (3) reveals that the effect of considering both SRH and Auger recombination instead of considering only SRH recombination becomes significant when S_n is lowered, when base width is decreased and when peak base doping level is increased. Figs. (4), (5) and (6) show the percentage difference or error introduced between these two considerations under three different circumstances.

Fig. (4) shows the percentage error under varying W_B for three different values of S_n. From this figure it has been observed that lowering of S_n causes the inclusion of Auger recombination in determining J_0 to be more significant. This is expected from the fact that the lowering of S_n reduces the surface recombination thereby causing volume recombination, especially, the Auger recombination to be dominant for high base doping levels. Moreover, increase in the base width increases the dominance of the Auger recombination for which % error is increased. This fact is also observed from Fig. (4). For a base with a width of 1 μm and a peak doping level of $5\times10^{19}\ cm^{-3}$, the % error is approximately 8% when $S_n = 3\times10^4\ cm/s$; the error is increased to as much as 22% when S_n is lowered to $S_n = 1\times10^4\ cm/s$. This observation is important. Efficiency for low-energy photon for a high-efficiency typical solar cell is $\approx$ 74% [13], which can be increased significantly by reducing the S_n and/or by increasing the base width. Since increasing the base width involves additional expenses for increasing amount of material, reduction of S_n is better choice to improve the low-energy photon efficiency and hence, to improve the conversion efficiency of modern solar cells.

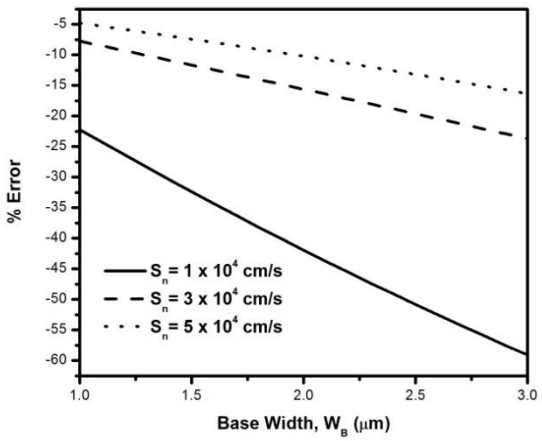

Figure 4: % error in base Saturation current density considering Auger recombination against the variation of base width for three values of surface recombination velocity ($S_n = 1\times10^4,\ 3\times10^4$ and 5×10^4 cm/sec.). Here, $N_a(W_B) = 5\times10^{19}\ cm^{-3}$.

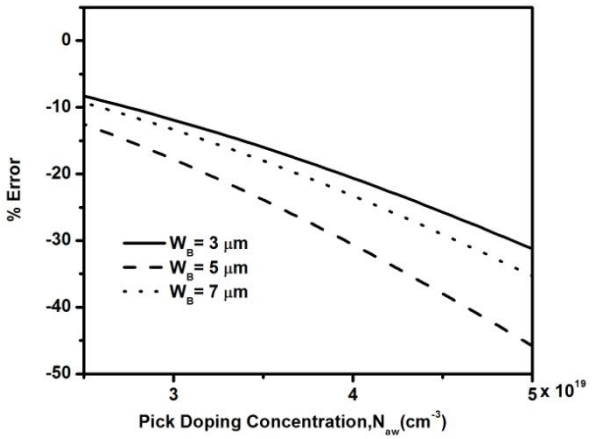

Figure 5: % error in base Saturation current density considering Auger recombination against the variation of peak base doping level for three values of base width ($W_B = 3,\ 5$ and $7\ \mu m$). Here, $S_n = 1\times10^5\ cm/sec$

Fig. (5) shows the percentage error under varying $N_a(W_B)$ for three different values of W_B. This figure shows that the effect of Auger recombination becomes dominant with the increase in $N_a(W_B)$. For a 3 μm wide base and with $S_n = 1\times10^5\ cm/s$, $N_a(W_B)$ of as high as $3\times10^{19}\ cm^{-3}$ can produce errors more than 10%. However, the use of such a high doping level in the p-type base region needs an explanation. Increase in the peak doping level keeping $N_a(0)$ constant increases the electric field in the base. This increased field decreases the diffusion current in the forward biased base region, which results in the increase of conversion efficiency. Additionally, high level doping in the base keeps the component of the series resistance in the base to a lower value. Therefore, the peak doping level as high as $3\times10^{19}\ cm^{-3}$ or higher is required to introduce in the base region to increase the conversion efficiency of the modern DF solar cells.

Fig. (6) shows that percentage error for varying $N_a(W_B)$ under three different values of S_n for a 3 μm wide base. This figure shows the dominance of Auger recombination when S_n is lowered or when $N_a(W_B)$ is increased. From this figure it is seen that the error introduced for the consideration of Auger recombination becomes more than 10% for a higher $N_a(W_B) = 5\times10^{19}\ cm^{-3}$ with higher $S_n = 5\times10^4\ cm/s$ and for a lower $N_a(W_B) = 2\times10^{19}\ cm^{-3}$ with lower $S_n = 1\times10^4\ cm/s$. However, it has been observed from Fig. (6) that the error is increased to as high as 60% for a $N_a(W_B) = 5 \times 10^{19}$ cm^{-3} with a $S_n = 1 \times 10^4$ cm/sec. This observaiton is important. Since the surface recombination velocity is considereably reduced in the present day solar cells and the peak doping level is required to increase to increase the conversion efficiency and since, the error introduced under such conditions goes up to 60% or higher, it can be concluded that the effects of Auger recombination must be included in the base saturation current modeling for the modern DF solar cells.

5. Conclusion

In this work, the effects of Auger recombination on the base dark saturation current density have been investigated and analyzed by developing an analytical model considering both SRH and Auger recombination mechanisms. The analytical intractability of the developed model has been resolved by employing an elegant exponential approximation technique. Simulation results obtained from the model under various considerations leads to the following important observations:

- Effect of Auger recombination becomes dominant when surface recombination velocity is lowered to the order of $10^4\ cm/s$.
- When the peak base doping level is increased to the order of $10^{19}\ cm^{-3}$, Auger recombination should be included in the modeling.
- Even for a very thin base (close to 1 μm), the effect of Auger recombination cannot be neglected, provided that the surface recombination velocity is lowered to $2\times10^4\ cm/s$ or less with a peak doping level increased to $2\times10^{19}\ cm^{-3}$ or higher.

These observations are very much important for modern drift solar cells, since these cells are required to fabricate with

thinner base with heavy doping level and also, with lowered surface recombination velocity for the considerable

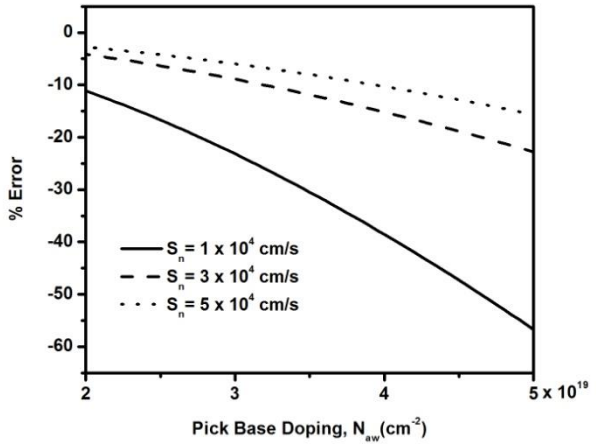

Figure 6: % error in base Saturation current density considering Auger recombination against the variation of peak base doping level for three values of surface recombination velocity ($S_n = 1\times10^4, 3\times10^4$ and 5×10^4 cm/sec). Here, $W_B = 3\mu m$.

improvement in the cell performance and the cell efficiency. Moreover, using the developed model in this work, the physics of various effects on the dark saturation current is readily understandable.

6. Appendix A: Exponential Approxımation Technique

Extending the idea suggested in the work [14], any exponential-like function f(x) defined in the region $0 < x < W$ can be approximated by a simple exponential function such that

$$f(x) \equiv F_0 e^{\frac{\eta_0}{W}} \tag{24}$$

where the logarithmic slope η can be obtained from the boundary values of f(x) as

$$\eta_0 = log\left[\frac{f(W)}{f(0)}\right] \tag{25}$$

and F_0 can be obtained from the fact that the areas under the original curve and the approximated curve must be equal

$$F_0 = \frac{\frac{\eta}{W}\int_0^W f(x)dx}{e^{\eta_0}-1} \tag{26}$$

The above-mentioned technique is termed in this work as "Exponential Approximation Technique". Applying this technique can significantly reduce the mathematical complexity without the loss of physical understanding.

6.1 Appendix B: Solution of the DE

Letting $n(x) = v(x)w(x)$ converts the second order differential equation (19) to

$$\frac{d^2v}{dx^2} + \left[\frac{2}{w}\frac{dw}{dx} + G_1\right]\frac{dv}{dx} + \frac{1}{w}\left[\frac{d^2w}{dx^2} + G_1\frac{dw}{dx} + G_2 w\right]v(x) = 0 \tag{27}$$

Letting $\frac{2}{w}\frac{dw}{dx} + G_1 = 0$, $w(x)$ can be obtained as

$$w(x) = e^{-\frac{1}{2}\int G_1(x)dx} = u^{-\frac{1-\gamma_2-\gamma_1}{2}} \tag{28}$$

Finally, letting $u^{k_n} = z^2$ transforms the Eqn (27) to a modified Bessel equation of order β as

$$\frac{d^2v}{dX^2} + \frac{1}{X}\frac{dv}{dX} - \frac{1}{X^2}\left(X^2+\beta^2\right)v = 0 \tag{29}$$

where $X = b_0 z$, $b_0 = \sqrt{R_0 F_e}\alpha_0$ and $\beta = \frac{1-\gamma_2+\gamma_1}{k_n}$. The solution n(x) can be expressed as

$$n(x) = w(x)\left[c_1 y_1(x) + c_2 y_2(x)\right] \tag{30}$$

where $y_1(x) = I_\beta(X)$ and $y_2(x) = K_\beta(X)$ are the modified Bessel function of the first kind and the second kind, respectively. Applying the required boundary conditions at $x = 0$ i.e. at the depletion edge and at $x = W_b$ i.e at the surface given by [6]

$$J_n(W_b) = -qS_n n(W_b) \text{ and } n(0) = \frac{n_{ie}^2(0)}{N_d(0)} e^{\frac{qV_L}{kT}}$$

C_1, C_2 can be obtained as

$$C_1 = \frac{n_w}{y_{1w} - \beta_s y_{2w}} \text{ and } C_2 = -\beta_s C_1$$

where $\beta_s = \frac{A_0 y_{10} + d y_{10}}{A_0 y_{20} + d y_{20}}$ and subscripts '0' and 'w' denotes the values at $x = 0$ and $x = W_b$.

References

[1] M. Wolf, "Drift fields in photovoltaic solar energy converter cells", *Proc. of the IEEE*,vol. 51, no. 5, pp. 674-693, May 1963.

[2] W. M. Bullis, "Influence of mobility and lifetime variations on drift-field effects in silicon-junction devices", IEEE Trans. Electron Devices, vol. 14, no. 2, pp. 75-81, February 1967.

[3] S. Kaye and G. P. Rolik, "Optimum bulk drift-field thicknesses in solar cells", IEEE Trans. Electron Devices, vol. 13, no. 7, pp. 563-570, July 1966.
[4] R. V. Overstraeten and W. Nuyts, "Theoretical investigation of the efficiency of drift-field solar cells", IEEE Trans. Electron Devices, vol. 16, no. 7, pp. 632-641, July1969.
[5] F. A. Lindholm and Y. H. Chen, "Current-voltage characteristic for bipolar p-n junction devices with drift fields, including correlation between carrier lifetimes and shallow-impurity concentration", J. App. Phys., vol. 53, no. 12, pp. 8863-8866, December 1982.
[6] Leendert A. Verhoff and Wim C. Sinke, "Minority-carrier transport in nonuniformly doped silicon-an analytical approach", IEEE Trans. Electron Devices, vol. 37, no. 1, pp. 210-221, January 1990.
[7] R. Burgers, "New Analytical Expression for Dark Current Calculation of highly doped region in semiconductor", IEEE Trans. Electron Devices, Jan. 1997, vol. 44, no. 1, pp. 171-179, January 1997.
[8] R. J. van Overstraeten, H. J. Deman and R. P. Mertens, "Transport equations in heavy doped silicon", IEEE Trans. Electron Devices, vol. ED-20, no. 3, pp. 290-298, March 1973.
[9] D. B. M. Klaassen, J. W. Slotboom and H. C. de Graaff, "Unified apparent bandgap narrowing in n- and p-type Silicon", Solid-State Electron, vol. 35, no. 2, pp. 125-129, February 1992.
[10] J. G. Fossum and D. S. Lee, "A physical model for the dependence of carrier lifetime on doping density in nondegenrate silicon", Solid-State Electron, vol. 25, no. 8, pp. 741-747, October 1982.
[11] J. G. Fossum, "Computer-aided numerical analysis of silicon solar cells", Solid-State Electron., vol. 19, no. 4, pp. 269-277, April 1976.
[12] J. Dziewior and W. Schmid, "Auger coefficient for highly doped and highly excited silicon", Appl. Phys. Lett., vol. 31, no. 5, pp. 346-348, May 1977.
[13] C. Hu and R. M. White, Solar Cells, McGraw-Hill Inc., New York, Figure 3.17,1983, pp. 61.
[14] Guoxin Li, Arnost Neugroschel, C. T. Sah, Don Hemmenway, Tony Rivoli and Jay Maddux, "Analysis of bipolar junction transistors with a Gaussian base-dopant impurity-concentration profile", IEEE Trans. Electron Devices, vol. 48, no. 12, pp. 2945-2947, December 2001.